

How Tomographic Cosmic Shear Maps Lead to Constraints on Dark Energy Properties

Hu Zhan* and Lloyd Knox†

Department of Physics, University of California, Davis, CA 95616

Using a number of numerical tests and analytic arguments we investigate *how* measurements of cosmic shear lead to constraints on dark energy. We find that, in contrast to the case with galaxy number density correlation functions, standard rulers in the matter power spectrum play no significant role. Sensitivity to distance ratios is provided by the ratios in the lensing kernel. An absolute distance scale can only be established by breaking a potential degeneracy between growth and distance which can be done if the growth-redshift relation and distance-redshift relations are parameterized with sufficiently few parameters. For the quality of dark energy determination, growth determination is primarily important because it improves the distance reconstructions. The information about dark energy in the growth-redshift relation is always of secondary importance though the amount it contributes is highly dependent on what priors are taken in the cosmological parameter space. We also explain the dependence of dark energy constraints from cosmic shear, relative distance measures (supernovae) and absolute distance measures (baryon acoustic oscillations) on assumptions about the mean curvature.

I. INTRODUCTION

The manner by which galaxy number density two-point correlation functions can be used to constrain dark energy is quite straightforward and well understood. In brief, the feature in the correlation function that arises from acoustic oscillations in the pre-recombination baryon- photon fluid is a standard ruler calibrated by cosmic microwave background (CMB) observations [1, 2, 3]. Detection of the angular extent of this feature (and/or redshift extent) at different redshifts allows for determination of the angular-diameter distance as a function of redshift, $D_A(z)$, (and/or expansion rate as a function of redshift, $H(z)$). The constraints on dark energy then follow from the dependence of these quantities on dark energy parameters. Similar statements could be made about the degree to which we understand the use of standard candles such as supernovae or standard populations such as clusters of galaxies — even though the latter is indeed a more complicated probe due to the dependence of the population statistics on the rate of growth $G(z)$ of large-scale structure.

In contrast, the manner by which cosmic shear two-point correlation functions constrain dark energy is not as straightforward nor is it as well understood. Others [4, 5, 6, 7] have already addressed this subject. Here we consider the question further. Whereas in [8] and [7] it was shown that one can reconstruct the distance-redshift and growth-redshift relations from cosmic shear data, here we explain *how* these functions are reconstructed. Whereas in [6] it was shown how information about relative distances could be extracted from cosmic shear data in a manner independent of assumptions about the matter power spectrum and its growth over time, here we

show how an *absolute* distance scale can be reconstructed as well, and discuss the model-dependence of the reconstruction. As in [4, 5, 6, 7] we comment further on the different roles played by growth-redshift and distance-redshift in constraining dark energy.

Baryon acoustic oscillations (BAOs) [e.g., 9, 10, 11, 12, 13] and weak lensing (WL) [e.g., 14, 15, 16, 17, 18, 19] are emerging as two promising probes of dark energy. Recent observations have detected the cosmic shear [20, 21, 22, 23, 24] and baryon wiggles [25, 26, 27, 28, 29], and they have been used to determine cosmological parameters such as the matter density and normalization of the matter power spectrum.

We know that WL surveys can constrain dark energy through the dependence of the distance-redshift relation and the growth-redshift relation on dark energy. Thus we begin by examining how these functions change as cosmological parameters are varied. We do so for both relative distance measures ($D_A(z)H_0$) and absolute distance measures ($D_A(z)$). Comparison between these two leads to an explanation of why Type Ia supernovae (SNe) are much more sensitive to assumptions about mean spatial curvature than is the case for BAOs.

In our effort to understand how WL constrains dark energy, we have found it useful to compare WL with what happens in the galaxy two-point correlation function case. There are two important differences between galaxy two-point correlation functions and shear two-point correlation functions. Shear two-point correlation functions do not depend on any unknown bias factor, and do depend on the ratio of distances in the lensing kernel. We find that both differences have a significant impact on dark energy constraints.

To assess the impact of the growth information obtainable due to the lack of an unknown bias factor, the impact of the distance dependence arising from the lensing kernel and various features in the power spectrum, we carry out a number of tests built upon a scale-free matter power spectrum and the normal cold dark matter (CDM)

*Electronic address: zhan@physics.ucdavis.edu

†Electronic address: lknox@ucdavis.edu

power spectrum with or without the baryon wiggles. We caution the reader that many systematic uncertainties are neglected in these tests in order to isolate the effect of the subject under investigation. Because of this, the results of these tests should not be taken as forecasts for future surveys.

One of the useful conclusions from our numerical tests is that power spectrum features play no significant role in WL-derived dark energy constraints, at least in the limit of infinite source density, i.e., no shot (shape) noise. We can thus discuss the response of shear power spectra to $D_A(z)$ and $G(z)$ using analytic expressions that simplify greatly for the case of power-law power spectra. In the presence of noise, changes to the power spectrum shape due to non-linear evolution boost the signal-to-noise ratio and thereby do lead to tighter constraints. For BAO, the nonlinear feature in the galaxy/matter power spectra can be a potential standard ruler for measuring the angular diameter distance. However, to take advantage of this prominent but evolving feature, one must model the nonlinearity and scale-dependent galaxy bias accurately.

We find that the sensitivity of WL to growth is mostly a nuisance. That is, the information about dark energy that can be inferred from constraints on the growth factor is subdominant to the dark energy information that can be inferred from distance constraints. The determination of the growth factor though, or more directly the amplitude of the power spectrum as a function of time, is important because it improves the distance determinations.

Throughout this paper, we assume a low-density CDM universe with the following parameters: the dark energy equation-of-state parameters w_0 and w_a as defined by $w(a) = w_0 + w_a(1 - a)$, the matter density ω_m , the baryon density ω_b , the angular size of the sound horizon at the last scattering surface θ_s , the equivalent matter fraction of curvature Ω_K , the optical depth to scattering by electrons in the reionized inter-galactic medium, τ , the primordial helium mass fraction Y_p , the spectral index n_s and running α_s of the primordial scalar perturbation power spectrum, and the normalization of the primordial curvature power spectrum Δ_R^2 at $k = 0.05 \text{ Mpc}^{-1}$. The fiducial values are taken from the 3-year *WMAP* data [30]: $(w_0, w_a, \omega_m, \omega_b, \theta_s, \Omega_K, \tau, Y_p, n_s, \alpha_s, \Delta_R^2) = (-1, 0, 0.127, 0.0223, 0.596^\circ, 0, 0.09, 0.24, 0.951, 0, 2.0 \times 10^{-9})$. The reduced Hubble constant $h = 0.73$ and the present equivalent matter fraction of dark energy $\Omega_X = 0.76$ are implicit in our parametrization.

The rest of the paper is organized as follows. §II examines the utility and reconstruction of distance and growth for studying dark energy. In §III, we compare cosmological constraints from BAO and WL obtained with various features in the matter power spectrum. We discuss the results and conclude in §IV.

II. PROBING DARK ENERGY WITH DISTANCE AND GROWTH

The relative strength of dark energy constraints from distance and growth is determined by two factors: the sensitivity to dark energy parameters and the precision with which they can be reconstructed. Since distance is more sensitive to the parameters [33] and since growth is determined several times worse than distance [7], the WL constraints on dark energy from the reconstructed distances are considerably stronger than those from the linear growth function [4, 7]. We note though that this conclusion is not reached consistently. Both [5] and [6] find the dark energy constraints from growth to be comparable to those from distance, as we will discuss below.

Distance and growth measurements in WL are entangled. For example, the precision on distance depends on how well one can measure the growth function. Hence, even if the growth function does not place very powerful constraints directly, being able to measure it well can still be crucial for probing dark energy.

A. Sensitivity

We show in Fig. 1 fractional changes of distance (left panel) and growth (right panel) with respect to a small deviation of the dark energy EOS parameters w_0 and w_a and the mean curvature parameter Ω_K from their fiducial values [see also 33, 34]. The fractional changes are calculated with all other parameters fixed. By holding ω_m , ω_b , and θ_s unchanged, one essentially fixes the comoving angular diameter distance to the last scattering surface D_A^* . The effect is that the fractional changes of the absolute comoving angular diameter distance D_A (lines in the left panel) vanish at $z \sim 1100$ and that $\Delta \ln D_A = \Delta \ln h$ at $z \sim 0$. One can measure the absolute distance with standard rulers such as BAOs. Since D_A is more sensitive to the mean curvature than to the dark energy EOS parameters, low- z BAO results could have strong dependence on the prior of Ω_K . As Fig. 1 suggests, high-redshift distances are efficient for measuring the mean curvature accurately as long as dark energy is subdominant at high redshift [35], which is indeed demonstrated in Ref. [36] for both photometric and spectroscopic BAO surveys. Therefore, it is helpful to extend BAO surveys to high redshift.

The behavior of $\Delta \ln D_A$ explains the “geometric degeneracy” between the mean curvature and Hubble constant for CMB results [30]. With a tight constraint on D_A^* from CMB and assuming $w = -1$, one then only needs an accurate measurement of the Hubble constant to determine the mean curvature. For example, with w fixed to -1 , $\sigma(\Omega_K) \sim |\sigma(\ln D_A) d\Omega_K/d \ln D_A|_{z \sim 0} \sim 0.12\sigma(\ln h)$. The current error of the Hubble constant is at 10% level [37], so we can infer that $\sigma(\Omega_K) \sim 10^{-2}$ with CMB and H_0 data alone, assuming $w = -1$.

Type Ia SNe measure the luminosity distance, which

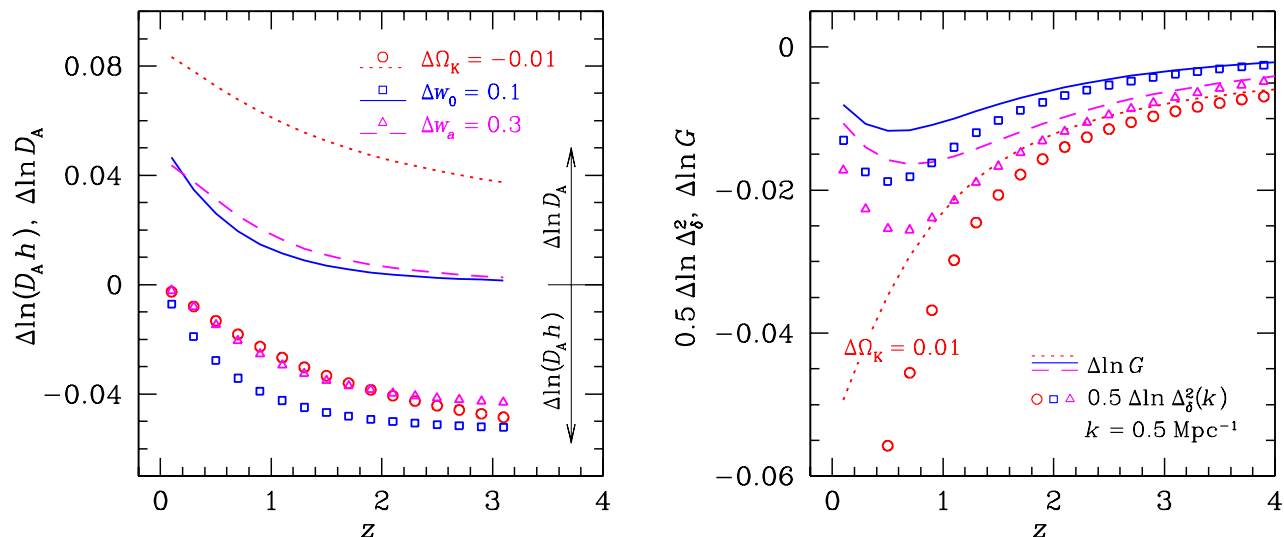


FIG. 1: *Left panel:* Fractional changes of the absolute comoving angular diameter distance D_A (lines) and the relative distance $D_A h$ (symbols) with respect to a small deviation of the dark energy EOS parameters w_0 and w_a and the mean curvature parameter Ω_K from their fiducial values. The fractional changes are calculated with all other parameters fixed. Fractional changes of the implicit Hubble constant equal $\Delta \ln D_A$ at $z \sim 0$ or $\Delta \ln(D_A h)$ at recombination. *Right panel:* Same as the left panel but for the linear growth function G (lines) and nonlinear growth at $k = 0.5 \text{ Mpc}^{-1}$ (symbols). The linear growth function follows the convention that $G(a) = a$ in an Einstein-de Sitter universe but $G(a = 1) \neq 1$ in general. The nonlinear linear matter power spectrum is obtained by applying the Peacock and Dodds [31] correction to the no-wiggle CDM power spectrum [32].

is the same as the angular diameter distance in comoving coordinates. Since the absolute luminosity of a SN is degenerate with the Hubble constant, SN distance is relative, i.e., one determines $D_A h$ instead of D_A . The fractional changes of $D_A h$ are given as symbols in the left panel of Fig. 1. One sees that the parameter sensitivity is shifted to higher redshift, which, counter-intuitively, leads to measuring the Hubble constant H_0 with high redshift data [34]. This is possible since the error in $D_A^* h$ is mostly from h . In practice, Ref. [38] finds that high redshift ($3 > z > 1.7$) SNe will not dramatically improve dark energy constraints, because with the extra data come new observational systematics, e.g., one may not even be able to obtain redshifts spectroscopically for these SNe.

The right panel of Fig. 1 shows that although the linear growth function (lines) is generally less sensitive to the dark energy EOS parameters and mean curvature than distance, nonlinear evolution (symbols) produces a marked amplification of the sensitivity [also noted in Ref. 5]. The growth function is more sensitive to the mean curvature than to the dark energy EOS parameters, and the sensitivity peaks at $z \sim 0$. As such, low redshift measurements of the growth function can be useful for constraining the mean curvature. One may also notice that the growth derivatives with respect to Ω_K , w_0 , and w_a have the same sign, whereas the distance derivatives do not. This breaks the degeneracy between the dark energy EOS parameters and mean curvature and is an advantage of being able to measure both distance and

growth well.

Figure 2 gives a demonstration of the importance of high-redshift distance measurements for BAO and low-redshift data for WL. We assume a half-sky photometric BAO and WL survey loosely based on the proposed Large Synoptic survey Telescope¹ (LSST) project. We use 10 WL bins over the photometric redshift range $0 \leq z_p \leq 3.5$ and 20 BAO bins over $0.15 \leq z_p \leq 3.5$. The widths of the WL bins are equal, while those of the BAO bins are proportional to $(1 + z_p)$. The linear galaxy bias is linearly interpolated over 20 bias parameters evenly distributed over true redshift $0 \leq z \leq 4$. The fiducial model for the galaxy bias is $b(z) = 1 + 0.84z$, and a 20% prior is applied to each bias parameter. The galaxy distribution is proportional to $z^2 \exp(-z/0.5)$ with a projected number density of 50 galaxies per square arcmin. The rms shear of the galaxies is taken to be $\gamma_{\text{rms}} = 0.18 + 0.042z$. To isolate the effects under investigation, we assume zero uncertainty in the error distribution of photometric redshifts which we take to be Gaussian with rms $\sigma_z = 0.05(1 + z)$ and bias $\delta z = 0$. The multipoles are limited to $40 \leq \ell \leq 3000$ for BAO [with an additional requirement that the dimensionless matter power spectrum $\Delta_g^2(k, z) < 0.4$] and $40 \leq \ell \leq 2000$ for WL. The calculation is performed with the forecasting tool CSWAB [33].

¹ See <http://www.lsst.org>.

We use the error product (EP), $\sigma(w_p) \times \sigma(w_a)$, to assess dark energy constraints. This product is proportional to the area of the error ellipse in the w_0 - w_a plane, and the error $\sigma(w_p)$ is equal to that on w_0 with w_a held fixed [39, 40, 41].

Because of the degeneracy between the galaxy bias and the growth of the large-scale structure, the BAO technique cannot measure the latter accurately even with the redshift distortion information in spectroscopic BAO data. This does not contradict the finding that one can determine the linear galaxy bias to several percent with BAO and CMB [33]. One might infer that the growth rate too could be determined to several percent as it is degenerate with the galaxy bias. However, the tight constraints on the linear galaxy bias are obtained with assumed cosmological dependence of the distance and growth function. If one models the distance and growth rate as independent free parameters, then the latter (or the product of the galaxy bias and growth rate) is poorly determined with BAO [42].

Photometric BAO (dotted line and open squares in Fig. 2), being only able to measure the absolute distance (and not the growth), is susceptible to the prior on the mean curvature, even though it is capable of determining Ω_K to 10^{-3} level with the full range of data [36]. This susceptibility is, however, much milder than that of relative distances from $z < 1.7$ SNe reported in Refs. [36, 43]. The degradation to the SN constraints due to relaxing the flatness assumption occurs mostly to w_a , because the redshift dependence of the derivative $d \ln(D_A h)/dw_a$ is nearly proportional to $d \ln(D_A h)/d\Omega_K$ (see Fig. 1). For BAO both w_0 and w_a are degraded, but the EP is degraded by much less than in the SN case.

The WL constraints (solid line and open circles in Fig. 2) on the dark energy EOS are remarkably robust against the flatness assumption, despite that the WL error on Ω_K is roughly twice that of BAO for LSST [33, 36]. To understand this behavior, we devise a test (dashed line and open triangles) in which we fix growth to the values it has in our fiducial model. In this case we can, on the one hand, reconstruct distance more accurately due to lack of any degeneracy with growth. On the other hand we lose any information about dark energy that comes through the dependence of the growth factor on dark energy. As expected, the dark energy constraints with only the distance information develop some sensitivity to the flatness assumption in this case. When the curvature is fixed to 0, the result of this test is fairly close to the normal WL ones especially at low redshifts where the growth rate is most sensitive to curvature. This shows that the (low- z) growth rate is helpful in reducing the error on curvature and, hence, improves the constraints on dark energy. However, it also illustrates that the power of WL comes mostly from the distance information.

A minor feature of the WL EP in Fig. 2 is that $z \gtrsim 2$ bins do not contribute much to the dark energy constraints, which is also seen for the mean curvature in Ref. [36]. This is mainly due to three factors. Firstly,

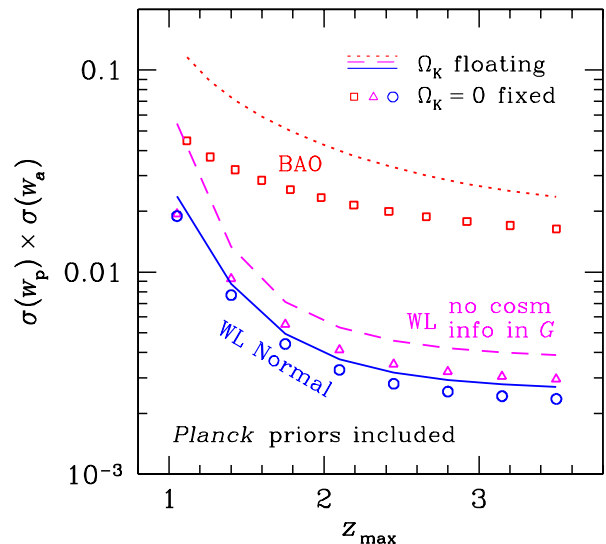


FIG. 2: Error product $\sigma(w_p) \times \sigma(w_a)$ as a function of the maximum (photometric) redshift of the data for BAO (dotted line and open square) and WL (solid line and open circles) with (symbols) and without (lines) the flatness assumption. The results are obtained by discarding BAO or WL bins above z_{\max} . In addition, we include the results of a test (dashed line and open triangles) in which we fix the growth rate to the values it has in our fiducial model.

the sensitivity of growth to the dark energy EOS and mean curvature peaks at low redshift. The peak of the lensing kernel moves away from the redshift range that is most sensitive to the parameters when the source galaxies are above $z \sim 2$. Secondly, WL is much more limited by shot noise than BAO [33], so that the poorer measurements at higher redshift contribute little to parameter constraints. If the shape noise were negligible for WL, the bins at $z \gtrsim 2$ would continue to improve the EP for bins at $z \lesssim 2$ by a factor of 2. In other words, one could see more improvement of WL constraints on dark energy at $z_{\max} \gtrsim 2$ with a deeper survey. Thirdly, we assume implicitly that dark energy is dominant only at low redshift with the parametrization w_0 and w_a (at the fiducial model $w_0 = -1$ and $w_a = 0$). If we allow more degrees of freedom in the dark energy EOS, e.g., by modeling it with 9 parameters evenly spaced between the expansion factor $a = 0.2$ and 1 [41], then high- z data will certainly be needed to constrain high- z dark energy.

B. Reconstructing Distance and Growth

We give a pedagogical explanation of how distance and growth are reconstructed from WL data in this subsection. For simplicity, we use a scale-free matter power spectrum with $d \ln P_\delta(k)/d \ln k = -2.5$ as an example. This is a good approximation since the WL technique does not rely on power spectrum features as we show in §III.

We begin by reviewing the dependence of the shear power spectra from two shear maps labeled by i and j and the gravitational potential power spectrum Δ_{Φ}^2 . For simplicity we assume all the source galaxies from which shear map i is derived are at the same redshift and distance, $D_i = D(z_i)$ and similarly for j (we drop the subscript A for convenience). In this case, and using the Limber approximation [44, 45] the 2-point function for the shear E modes in a flat universe is given by [16, 46]

$$P_{ij}^{\gamma\gamma}(\ell) = \int dD \frac{D_i - D}{D_i} \frac{D_j - D}{D_j} [k\Delta_{\Phi}^2(k, z)]_{k=\ell/D} \times \Theta(D_i - D)\Theta(D_j - D), \quad (1)$$

where z in square brackets corresponds to the redshift of the comoving angular diameter distance $D(z)$, and $\Theta(x)$ is the Heaviside step function.

The potential power spectrum is related to the matter power spectrum by $k\Delta_{\Phi}^2(k) = \frac{9}{8\pi^2} (\Omega_m H_0^2)^2 / a^2 P_{\delta}(k)$. Although $P_{\delta}(k)$ is not a power law (this is the evolved matter power spectrum at late times, not the primordial power spectrum) insight can be gained by considering the power law case. If $P_{\delta}(k, z) = Ak^n g_{\Phi}^2(D)/a^2$, where $g_{\Phi}(D) = G(z)/(1+z)$ is the gravitational potential growth factor at the redshift corresponding to the comoving angular distance $D(z)$, then

$$P_{ij}^{\gamma\gamma}(\ell) = A'\ell^n \int \frac{dD}{D} \frac{D_i - D}{D_i} \frac{D_j - D}{D_j} D^{1-n} g_{\Phi}^2(D) \times \Theta(D_i - D)\Theta(D_j - D), \quad (2)$$

where A' is an easily derived constant.

We see that in the power law power spectrum case, there is no information about geometry in the shape of the shear power spectra since the shape only depends on the spectral index. Any information about geometry is in the amplitudes of the various shear power spectra, which are also affected by the growth function. Therefore we can count parameters and degrees of freedom to gain an understanding of the reconstruction of distance and growth. If we assume m shear maps and parameterize both the $D(z)$ function and the $g_{\Phi}(z)$ function with m parameters each, as was done in Ref. [7], then there are $m(m+1)/2$ knowns (the amplitudes of each of the shear power spectra) and $2m$ variables to solve for. For $m > 2$ the known quantities are more numerous than the unknown and generally there is a unique least-square solution. For a reconstruction of the parameters of a physical model from several source redshift bins, typically the number of knowns exceeds the number of parameters.

Note that if we were to consider $g_{\Phi}(D)$ to be a completely free function, then knowledge of absolute distances would be impossible to acquire since a rescaling of distance would be exactly degenerate with a rescaling of $g_{\Phi}(D)$. Also, for the special case of $n = 1$ (which is only a good approximation at $\ell \lesssim 30$) there is no sensitivity to absolute distances even with $g_{\Phi}(D)$ perfectly known. Fortunately, $n = -2.5$ is a better approximation

to the shear power spectrum over most of the ℓ -range of interest, providing a strong sensitivity to the absolute distance scale when $g_{\Phi}(D)$ is parameterized with just a few numbers.

We can further simplify things by replacing the integral over distance in Eq. (1) for the auto shear power spectra with the integrand evaluated at an effective lens redshift z_1 with width ΔD_1 , so that

$$P_{ii}^{\gamma\gamma}(\ell) \propto \Delta D_1 D_{1i}^2 D_i^{-2} P_{\delta}(k, z_1) \propto D_{1i}^2 D_i^{-2} D_1^{2.5} G_1^2, \quad (3)$$

where D_{1i} is the comoving angular diameter distance between the lens and the source bin i , $G_1 = G(z_1)$, and $P_{\delta}(k, z_1) \propto G_1^2 k^{-2.5}$.

If one models D_i , D_{1i} , D_1 , and G_1 as independent parameters, then these parameters will have roughly the same fractional error because of the similar magnitude of exponents. The errors of these parameters will be highly correlated. Since a lens distance for one WL bin can become a source distance for another and vice versa, the same distance is measured by multiple (auto and cross) shear power spectra. The degenerate directions of the distances for different shear power spectra can be quite complementary to each other. Therefore, the tomographic WL reconstruction of distance is more accurate than that of growth. The degeneracy may be partially lifted by the cosmological model as well. For example, the distance $D_{1i} = D_i - D_1$ in a flat universe.

The reconstructed distances (and growth rates) from WL are still highly correlated, but the degeneracies are along directions that cannot be easily mimicked by cosmological parameters. This is why even though the distances reconstructed with LSST BAO [42] have smaller marginalized errors than those with LSST WL [7], the dark energy constraints from the former is nevertheless weaker (note that the growth information itself contributes only in a minor way, see Fig. 2).

For comparison, the angular galaxy power spectra with the same approximation are

$$P_{ii}^{\text{gg}}(\ell) \propto D_i^{0.5} b_i^2 G_i^2, \quad (4)$$

where b_i is the linear galaxy bias. Since the galaxy power spectra, unlike WL shear power spectra, are local to the underlying galaxy distribution, i.e., no mixing of distances at other redshifts in Eq. (4), one cannot measure the same distance multiple times with different auto and cross galaxy power spectra to break the degeneracies and reduce the errors. The exponents of D_i , b_i , and G_i in Eq. (4) suggest that, with distances measured from the BAO feature, one can then infer from P_{ii}^{gg} the product $b_i G_i$ with one fourth the fractional distance error. In the case that growth is constrained tightly from (a combination with) other data (WL for example) and a physical model, then the bias parameter can be determined quite precisely as was seen in Refs. [33, 40].

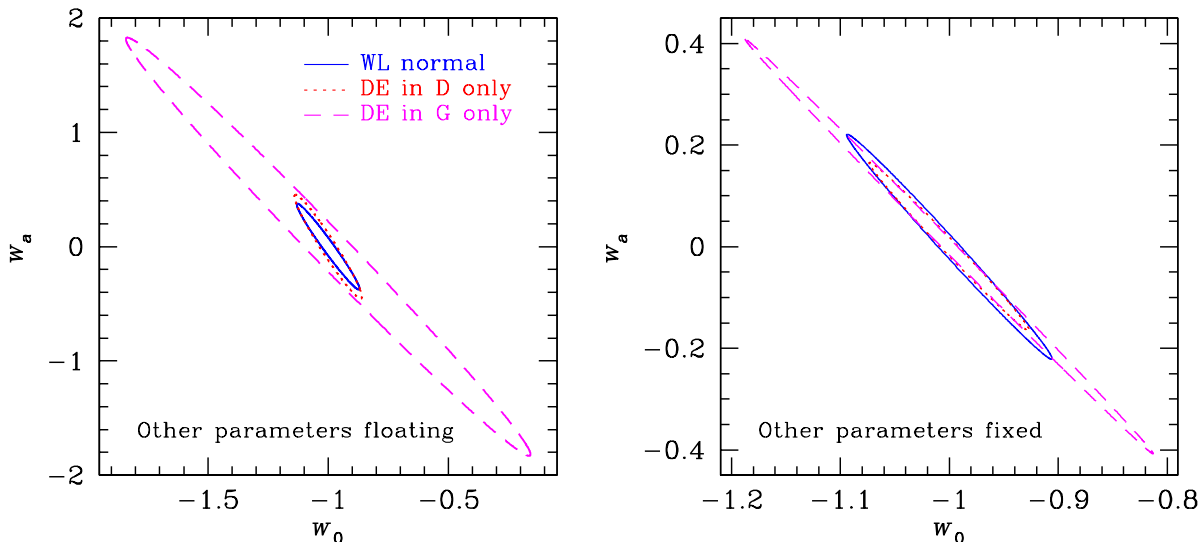


FIG. 3: *Left panel*: 1σ error contours in the w_0 - w_a plane for normal WL (solid lines), WL with dark energy information in the growth rate discarded (dotted line), and WL with dark energy information in the distance discarded (dashed line). The results are marginalized over all the other cosmological parameters. *Right panel*: Same as the left but with all the other parameters fixed. The distance-only contour is slightly smaller than the normal WL contour in this panel because of the partial cancellation between the distance and growth effects [5].

C. Dark Energy Constraints from Distance and Growth

We examine the relative strength of dark energy constraints from the distance and growth rate with the WL technique. In the same spirit as the test in Fig. 2, we evaluate the dark energy constraints from the distance by not allowing the growth to depend on dark energy parameter variations (“DE in D only”) and vice versa (“DE in G only”). We take independent Gaussian priors for the tests: $\sigma_P(\ln \omega_m) = \sigma_P(\ln \omega_b) = \sigma_P(n_s) = \sigma_P(\alpha_s) = \sigma_P(\ln \Delta_R^2) = 0.05$, $\sigma_P(\theta_s) = 0.003^\circ$, $\sigma_P(\tau) = 0.01$, and $\sigma_P(Y_p) = 0.02$. These priors are fairly conservative compared to what can be achieved with *Planck*, and they do not introduce extra correlations between the parameters.

The results are shown in Fig. 3. When marginalized over all the other cosmological parameters (left panel), the distance (dotted line) is far more powerful than the growth rate (dashed line), and the WL constraints on dark energy (solid line) are almost entirely from the distance. This is consistent with the conclusions in Refs. [4, 7]. The difference between the constraints from the distance and growth rate depends on the priors on the other parameters. If one fixes all the other parameters (right panel), then the distance and growth rate offer comparable dark energy constraints, in agreement with Refs. [5, 6].

Note that, as can be seen in Fig. 3, the constraints on dark energy are tighter in the “DE in D only” case than in the “WL normal” case. This is because there are two effects of fixing G with respect to dark energy variations. One effect is that one now has better distance information because there is no degeneracy with growth. The other,

apparently subdominant effect, is the loss of any information that comes through the dependence of growth on dark energy. The improvement in the artificial case of ignored growth dark energy dependence is also consistent with the notion that there is a partial cancellation of the effects on the shear power spectra of varying distance and growth through the dark energy EOS [5].

D. Why Does WL Perform Better than BAO?

We now get at the question of how WL surveys constrain dark energy by comparing them with BAO surveys. There are two major differences between the two probes. First, there is an unknown bias that affects the galaxy power spectra. The bias means that growth information is not accessible, since growth and bias are degenerate. Also due to the bias, analysis of galaxy power spectra is typically restricted to mostly linear scales to avoid the complications of a scale-dependent bias (besides nonlinear evolution of the matter power spectrum itself). Second, the kernels are different. The WL kernel is broader, suppressing sensitivity to matter power spectrum features, and it also depends on distances, making the amplitude of the shear power spectra sensitive to the distance-redshift relation.

We can gain insight by comparing a WL survey to something even better than a galaxy survey: a map of the dark matter density as a function of redshift and angular coordinates, with no peculiar velocity contributions to the redshifts. Would such a survey be better than a WL survey at determining dark energy parameters? One might think so since the shear maps are merely projec-

tions over this density field, projections that will suppress the prominence of power spectrum features. However, our tests in the next section show that the WL survey is significantly more constraining. The reason is that the projection is dependent on the distance-redshift relation and, in fact, is the main source of sensitivity of the shear power spectra to the distance-redshift relation.

Thus our conclusion is that while the lack of any unknown bias factor may be important, it is not the crucial difference between WL and galaxy surveys. The WL kernel is the most important difference.

The bias factor is indeed an important difference as well. If WL were affected by an unknown bias factor that was a free function of redshift, then the constraints on dark energy would be greatly degraded. In apparent contradiction we have also seen that the constraints on dark energy from the growth information are highly subdominant to those from distance information. These two statements are both true. The reason an unknown bias factor would degrade the dark energy constraints is not due to the loss of growth information, but because without priors on the growth of the gravitational potential as a function of redshift, the distance reconstruction degrades.

In fact, if we let growth be a free function, this would be the same as letting the bias be a free function. The quality of the distance reconstruction from WL depends on the growth-redshift relation having a sufficiently small number of parameters — whether those are the parameters of the cosmological model or the parameters of a phenomenological model such as the growth factor evaluated at a discrete set of points in redshift space, as was done in Refs. [8] and [7] and as was discussed above.

Finally, we should be clear that although WL gets tighter constraints on the distance-redshift relation than BAO, this is not necessarily apparent from looking at the errors on the distances to particular redshifts. The BAO ones can be smaller. However, the errors in the distances to particular redshifts in the WL case are highly correlated with the errors in the distances to other redshifts. Because of these correlations, there are linear combinations of distances with much smaller errors than any individual distance. These strong correlations are present because any single auto or cross shear power spectrum depends on the distance to many redshifts.

III. POWER SPECTRUM FEATURES AND COSMOLOGICAL CONSTRAINTS

We devise a number of tests to explore the impact of power spectrum features, such as the broadband turnover, BAOs, and nonlinear evolution, on the constraints of dark energy and related cosmological parameters. The tests are divided into two broad categories: with and without the shot noise. The former has the advantage that the overall amplitude of the signal, i.e., the normalization of the galaxy or shear power spectra,

TABLE I: Convention of test names.

Prefix	Feature	Suffix	Feature
SF	scale-free ^a	LE	linear evolution
NW	no wiggle ^b	NE	nonlinear evolution
WW	with wiggle ^c	SR	artificial standard ruler
		AB	artificial bias for WL
		FB	fixed bias for BAO

^aWith the spectral index $d \ln P(k)/d \ln k = -2.5$ and amplitude proportional to that of the CDM power spectrum.

^bGiven by the fitting formula in Ref. [32].

^cCalculated with CMBFAST [47].

does not affect the Fisher matrix for error estimation. In other words, only the power spectrum shapes and their relative amplitudes affect the constraints when the shot noise is neglected. Clearly, the noise-free case is unrealistic. The inclusion of the shot noise degrades the results (more severely for WL), and in this case a boost to the power spectrum and its sensitivity to parameters due to nonlinear evolution can be helpful.

We use a scale-free matter power spectrum, a CDM power spectrum with no baryon wiggles, and a CDM power spectrum with wiggles to carry out the tests. For each type, we specify up to 5 additional characteristics: linear evolution, nonlinear evolution, artificial standard ruler on nonlinear scales, artificial bias for WL, and fixed galaxy bias for BAO. Table I summarizes the convention of test names; for example, NWLE refers to the no-wiggle CDM power spectrum that evolves according to the linear theory on all scales.

Note that linear evolution applies to all cases unless nonlinear evolution is specified. For SFNE and WWNE, the relative boost to the matter power spectrum due to nonlinear evolution is set to be the same as that of NWNE, in order to avoid the difficulty of applying the Peacock and Dodds [31] fitting formula for the nonlinear power spectrum to the CDM power spectrum with wiggles [33]. In addition, using the same relative boost of the power spectrum ensures the same parameter sensitivity arising from the nonlinear correction.

The artificial standard ruler is given by

$$\frac{P_{\text{SR}}(k)}{P_{\delta}(k)} = 1 + 9 \left(1 - e^{-u^2}\right) + 9\sqrt{q} \left(1 - e^{-v^2}\right), \quad (5)$$

where $q = k/(h \text{Mpc}^{-1})$, $u = q/1.5$, and $v = q/3$. This feature mimics the Peacock and Dodds [31] fitting formula of the nonlinear matter power spectrum for our fiducial cosmological model at $z = 0$. Its independence of redshift makes the artificial feature standard and, meanwhile, stronger than nonlinear evolution at $z > 0$. Since we impose the condition $\Delta_{\delta}^2(k, z) < 0.4$ and $40 \leq \ell \leq 3000$ for galaxy power spectra, the artificial standard ruler and nonlinear evolution affect our analysis only through their influence on larger scales. The artificial bias for WL is implemented in the same way as the galaxy bias but with a fiducial model of $b = 1$. A

TABLE II: Parameter errors from noise-free galaxy power spectra.

Case	w_p	w_a	$\ln \omega_m$	Ω_K	$\ln \Delta_R^2$
			(10^{-2})		
SFLE	2.3	14	5.0	13	5.0
SFNE	0.18	1.6	2.2	1.3	4.9
SFSR	0.037	0.81	4.6	0.98	4.9
SFFB	0.032	0.25	2.6	0.41	4.3
SFFB ^a	0.019	0.13	2.6	0.37	4.3
NWLE	0.11	1.5	3.5	0.95	4.8
NWNE	0.11	1.4	3.6	0.61	4.8
NWSR	0.037	0.85	3.8	0.87	4.8
NWFB	0.018	0.12	3.3	0.38	2.1
NWFB ^a	0.012	0.10	2.8	0.38	1.3
WWLE	0.034	0.58	2.7	0.22	4.8
WWNE	0.035	0.51	2.2	0.21	4.8
WWFB	0.012	0.08	2.4	0.20	1.9
WWFB ^a	0.010	0.07	2.5	0.25	1.9

^aThese FB results are calculated in the same way as the WL ones in Table III, i.e., with 10 uniform bins and $40 \leq \ell \leq 2000$ without a limit on $\Delta_s^2(k, z)$.

20% prior on the galaxy and artificial bias parameters is always applied.

A. Noise-Free Case

Since BAO and WL are not sensitive enough to all the parameters (e.g., the electron optical depth of the reionized intergalactic medium), at least some parameter priors are needed to regularize the constraints [19]. The correlation of parameters in CMB priors can obscure the effect of power spectrum features we try to isolate. Hence, in the noise-free case we take the same independent Gaussian priors as those in Fig. 3.

Table II presents the marginalized errors on w_p , w_a , ω_m , Ω_K , and Δ_R^2 from noise-free angular galaxy power spectra with various underlying matter power spectra. As we expect, SFLE does not provide meaningful constraints on the parameters, because it has no feature for measuring the absolute distance and because the galaxy bias prevents one from extracting the distance and growth information from the amplitude of the galaxy power spectra. The redshift-dependent, but predictable, ruler provided by nonlinear evolution leads to an improvement of SFNE over SFLE. However, the length of this ruler cannot be predicted very accurately since it depends on both the shape and amplitude of the matter power spectrum. Therefore when other rulers are present, the addition of nonlinear evolution makes very little difference, as in the case of NWNE vs. NWLE and WWNE vs. WWLE. We should point out that the tests in Table II do not take full advantage of the nonlinear evolution as we truncate the matter power spectrum at

TABLE III: Parameter errors from noise-free shear power spectra.

Case	w_p	w_a	$\ln \omega_m$	Ω_K	$\ln \Delta_R^2$
			(10^{-2})		
SFLE	0.0032	0.023	1.9	0.19	3.5
SFNE	0.0034	0.027	1.5	0.14	2.7
SFSR	0.0031	0.022	1.9	0.18	3.4
SFAB	0.014	0.16	4.2	0.56	4.7
NWLE	0.0036	0.021	2.1	0.17	1.1
NWNE	0.0035	0.026	2.1	0.14	0.37
NWSR	0.0030	0.022	2.0	0.16	1.1
NWAB	0.013	0.13	2.5	0.50	4.5
WWLE	0.0033	0.020	1.9	0.16	1.3
WWNE	0.0033	0.025	1.2	0.13	0.78
WWAB	0.0089	0.072	2.6	0.30	4.5

largely linear scales. Extending the analysis to smaller scales does increase the difference between WWLE and WWNE results (see § III B), but doing so requires one to model the scale-dependent galaxy bias on those scales very accurately.

The artificial standard ruler of Eq. (5) is similar to the nonlinear feature at $z = 0$ but independent of redshift. It offers a great improvement on distance measurements over SFNE, which is evident from the errors on w_p , w_a , and Ω_K , but, having nothing to do with ω_m , it does not reduce $\sigma(\ln \omega_m)$. When the galaxy bias is fixed in SFFB, the distance and growth can be measured through the amplitudes of the galaxy power spectra, which have distance dependencies and lead to the smallest errors on nearly all parameters within the SF group. One still cannot do well on Δ_R^2 with SFFB, because the normalization of growth and that of distance are degenerate for scale-free galaxy power spectra. The sensitivity of SFFB to ω_m comes from our choice of normalizing the matter power spectrum to the CMB potential fluctuations [33].

With the standard ruler of the broadband turnover in the matter power spectrum, NWLE performs much better than SFLE, and nonlinear evolution becomes a subdominant factor. As in SFSR, the artificial standard ruler in NWSR offers yet better measurements of the absolute distance and stronger constraints on parameters. Because of the broadband turnover, a shift in the absolute distance will not only alter the amplitude of the angular galaxy power spectra but also move the broadband feature in multipole space. This breaks the degeneracy between the normalizations of growth and distance seen in SFFB, so that NWFB improves Δ_R^2 (in addition to other parameters) significantly.

By comparing the results of the NW tests and those of the WW tests, one sees that the BAOs are by far the most crucial feature for measuring the absolute distance and constraining cosmology with galaxy power spectra. Their importance relative to that of the broad band feature was already convincingly demonstrated by Ref. [13].

Also, WWFB demonstrates that it would be highly advantageous to be able to predict the bias to high precision since the results improve dramatically for fixed galaxy bias.

Table III gives the results from the noise-free WL shear power spectra. The most striking characteristic is that these results are fairly independent of all our modeling changes, except for the introduction of artificial bias. There is no substantial difference between the dark energy constraints from completely featureless SFLE and those from WWNE. The larger errors on Δ_R^2 with the scale-free matter power spectrum is due to the degeneracy between the normalization of distance and that of growth, as is the case in Table II. This shows that the WL constraints on dark energy are primarily derived from the correlated distances, which are inferred from the amplitudes of the shear power spectra. One would not obtain the same distance constraints without the ability to measure the growth function. This is illustrated by the severe degradation to the results of SFAB, NWAB, and WWAB for which the lensing potential is artificially sourced by unknown bias parameters [see also 36]. One may notice among the AB tests that WWAB is considerably better than the other two as far as w_0 and w_a are concerned. This reveals that the standard features in the matter power spectrum do contribute somewhat to WL constraints on dark energy, but they are much less important than the lensing kernel and the lack of bias in the WL technique.

It is also of interest to compare the results of SFFB in Table II with those of SFLE in Table III. In the noise-free case, the errors of the shear power spectra and those of the galaxy power spectra are given identically by the cosmic variance. For the same scale-free matter power spectrum and fixed galaxy bias, Eqs. (3) and (4) predict a stronger sensitivity of shear power spectra to distances than is the case for galaxy power spectra. Thus we expect to have tighter constraints on distances from shear power spectra than from galaxy power spectra, although the former will probably have a more complicated error correlation structure. The expectation of tighter constraints is indeed supported by the much smaller errors on w_p and w_a from SFLE in Table III compared to those from SFFB in Table II.

B. Constraints with the shot noise

The noise-free tests in the previous sub-section are useful for understanding the origins of cosmological constraints for the BAO and WL techniques, though the constraints can behave quite differently with noise. To evaluate the effect of nonlinear evolution more realistically, we include the shot noise and apply CMB priors from *Planck* to the tests in Table IV.

Compared to the results in Table II, the shot noise increases the BAO EP, $w_p \times w_a$, only mildly. The improvement to other parameters is due to the *Planck* pri-

TABLE IV: Cosmological constraints from galaxy and shear power spectra with the shot noise and *Planck* priors.

Case	Probe	w_p	w_a	$\ln \omega_m$	Ω_K	$\ln \Delta_R^2$
				(10^{-2})		
WWLE	BAO	0.037	0.66	0.50	0.11	1.8
WWNE	BAO	0.040	0.59	0.51	0.10	1.8
WWLE ^a	BAO	0.027	0.49	0.50	0.099	1.8
WWNE ^a	BAO	0.028	0.38	0.48	0.089	1.8
WWLE	WL	0.019	0.23	0.84	0.22	1.8
WWNE	WL	0.014	0.19	0.67	0.19	1.7

^aThese BAO results are obtained with wider range of scales by relaxing $\Delta_\delta^2(k, z)$ to less than unity instead of $\Delta_\delta^2(k, z) < 0.4$.

ors. The inclusion of nonlinear evolution decreases BAO EP by merely 2%, because we only use the galaxy power spectra on largely linear scales. If we extend the scales of the analysis by relaxing $\Delta_\delta^2(k, z)$ to less than unity (instead of $\Delta_\delta^2(k, z) < 0.4$), the improvement on the EP due to the nonlinear feature elevates to 20%. However, it may be quite optimistic as we have not accounted for our uncertain knowledge of the scale-dependent galaxy bias in the quasi-linear regime.

Unlike BAO, the WL technique is more limited by the shot noise, so that the results in Table IV are a lot worse than those in Table III. In other words, the WL constraints should be sensitive to nonlinear evolution, which boosts the shear power spectra on scales where the shot noise is dominant. Hence, the WWNE WL constraints are considerably tighter than the WWLE WL constraints in Table IV, even though WL results can be degraded by nonlinear evolution in the noise-free case.

IV. CONCLUSIONS

The dependence of WL shear power spectra on $D(z)$ and $G(z)$ is much more complicated than, say, that of supernova luminosity distance. Here we have employed a number of numerical tests and analytic arguments to gain an understanding of *how* WL observations recover information about $D(z)$ and $G(z)$ and thus constrain cosmology and dark energy in particular. We have also similarly explored the cosmological constraints from the correlations of number densities of galaxies in photometric redshift bins.

We have found that, in contrast to the case with galaxy correlations, standard rulers in the matter power spectrum play no significant role in $D(z)$ reconstruction from WL surveys. Instead, the dependence of the lensing kernel on distance ratios allows for a determination of the distance ratios. Furthermore, the shear power spectra are directly connected to the matter power spectrum without any bias, so that one can determine the degenerate normalizations of distance and growth from the amplitude of

the shear power spectra. This degeneracy can be broken by assuming a physical model for either quantity, which occurs, for example, when one projects the constraints on distances and growth rates into cosmological parameter space. With WL, the growth information itself is less powerful than the distance information in constraining dark energy. However, as mentioned in § I, it is crucial to have the ability to measure the amplitude of the matter power spectrum. Otherwise, the WL technique would achieve much lower precision on the distance-redshift relation and therefore much lower precision on cosmological parameters as well.

With galaxy power spectra if there were no confusion from the galaxy bias then knowing the amplitude of the matter power spectrum would also help in determining the distance-redshift relation from the amplitude of the galaxy power spectra. We find that the ruler from non-linear evolution, due to its redshift and model dependencies, is more difficult to standardize than other features

in the matter power spectrum such as the BAOs. It will not help with constraints from galaxy power spectra unless the scale-dependent galaxy bias can be modeled very well.

We expect this understanding of how galaxy surveys constrain cosmology (via WL in particular) to be useful for analytic consideration of various effects such as systematic errors, enlarged cosmological parameter spaces, and the inclusion of complementary information.

Acknowledgments

We thank J. A. Tyson for helpful comments on the manuscript and A. J. Hamilton for a useful conversation. This work was supported by NASA grant NAG5-11098 and NSF grants No. 0307961 and 0441072.

-
- [1] P. J. E. Peebles and J. T. Yu, *Astrophys. J.* **162**, 815 (1970).
- [2] J. R. Bond and G. Efstathiou, *Astrophys. J. Lett.* **285**, L45 (1984).
- [3] J. A. Holtzman, *Astrophys. J. Suppl. Ser.* **71**, 1 (1989).
- [4] K. Abazajian and S. Dodelson, *Physical Review Letters* **91**, 041301 (2003).
- [5] F. Simpson and S. Bridle, *Phys. Rev. D* **71**, 083501 (2005).
- [6] J. Zhang, L. Hui, and A. Stebbins, *Astrophys. J.* **635**, 806 (2005).
- [7] L. Knox, Y.-S. Song, and J. A. Tyson, *Phys. Rev. D* **74**, 023512 (2006).
- [8] Y.-S. Song, *Phys. Rev. D* **71**, 024026 (2005).
- [9] D. J. Eisenstein, W. Hu, and M. Tegmark, *Astrophys. J. Lett.* **504**, L57 (1998).
- [10] C. Blake and K. Glazebrook, *Astrophys. J.* **594**, 665 (2003).
- [11] W. Hu and Z. Haiman, *Phys. Rev. D* **68**, 063004 (2003).
- [12] E. V. Linder, *Phys. Rev. D* **68**, 083504 (2003).
- [13] H. Seo and D. J. Eisenstein, *Astrophys. J.* **598**, 720 (2003).
- [14] W. Hu and M. Tegmark, *Astrophys. J. Lett.* **514**, L65 (1999).
- [15] Y. Mellier, *Annu. Rev. Astron. Astrophys.* **37**, 127 (1999), astro-ph/9812172.
- [16] M. Bartelmann and P. Schneider, *Phys. Rep.* **340**, 291 (2001).
- [17] D. Huterer, *Phys. Rev. D* **65**, 063001 (2002).
- [18] A. Refregier, *Annu. Rev. Astron. Astrophys.* **41**, 645 (2003).
- [19] Y.-S. Song and L. Knox, *Phys. Rev. D* **70**, 063510 (2004).
- [20] D. J. Bacon, A. R. Refregier, and R. S. Ellis, *Mon. Not. R. Astron. Soc.* **318**, 625 (2000).
- [21] D. M. Wittman, J. A. Tyson, D. Kirkman, I. Dell’Antonio, and G. Bernstein, *Nature (London)* **405**, 143 (2000).
- [22] L. Van Waerbeke, Y. Mellier, M. Radovich, E. Bertin, M. Dantel-Fort, H. J. McCracken, O. Le Fèvre, S. Foucaud, J.-C. Cuillandre, T. Erben, et al., *Astron. Astrophys.* **374**, 757 (2001).
- [23] M. Jarvis, G. M. Bernstein, P. Fischer, D. Smith, B. Jain, J. A. Tyson, and D. Wittman, *Astron. J.* **125**, 1014 (2003).
- [24] H. Hoekstra, Y. Mellier, L. van Waerbeke, E. Semboloni, L. Fu, M. J. Hudson, L. C. Parker, I. Tereno, and K. Benabed, *Astrophys. J.* **647**, 116 (2006), astro-ph/0511089.
- [25] S. Cole, W. J. Percival, J. A. Peacock, P. Norberg, C. M. Baugh, C. S. Frenk, I. Baldry, J. Bland-Hawthorn, T. Bridges, R. Cannon, et al., *Mon. Not. R. Astron. Soc.* **362**, 505 (2005).
- [26] D. J. Eisenstein, I. Zehavi, D. W. Hogg, R. Scoccimarro, M. R. Blanton, R. C. Nichol, R. Scranton, H.-J. Seo, M. Tegmark, Z. Zheng, et al., *Astrophys. J.* **633**, 560 (2005).
- [27] C. Blake, A. Collister, S. Bridle, and O. Lahav, *ArXiv Astrophysics e-prints* (2006), arXiv:astro-ph/0605303.
- [28] G. Hütsi, *Astron. Astrophys.* **449**, 891 (2006).
- [29] N. Padmanabhan, D. J. Schlegel, U. Seljak, A. Makarov, N. A. Bahcall, M. R. Blanton, J. Brinkmann, D. J. Eisenstein, D. P. Finkbeiner, J. E. Gunn, et al., *ArXiv Astrophysics e-prints* (2006), arXiv:astro-ph/0605302.
- [30] D. N. Spergel, R. Bean, O. Dore’, M. R. Nolta, C. L. Bennett, G. Hinshaw, N. Jarosik, E. Komatsu, L. Page, H. V. Peiris, et al., *ArXiv Astrophysics e-prints* (2006), arXiv:astro-ph/0603449.
- [31] J. A. Peacock and S. J. Dodds, *Mon. Not. R. Astron. Soc.* **280**, L19 (1996).
- [32] D. J. Eisenstein and W. Hu, *Astrophys. J.* **511**, 5 (1999).
- [33] H. Zhan, *Journal of Cosmology and Astro-Particle Physics* **8**, 8 (2006), astro-ph/0605696.
- [34] W. Hu, in *ASP Conf. Ser. 339: Observing Dark Energy*, edited by S. C. Wolff and T. R. Lauer (2005), pp. 215–+.
- [35] L. Knox, *Phys. Rev. D* **73**, 023503 (2006).
- [36] L. Knox, Y.-S. Song, and H. Zhan, *ArXiv Astrophysics e-prints* (2006), arXiv:astro-ph/0605536.
- [37] W. L. Freedman, B. F. Madore, B. K. Gibson, L. Ferrarese, D. D. Kelson, S. Sakai, J. R. Mould, R. C. Ken-

- nicutt, H. C. Ford, J. A. Graham, et al., *Astrophys. J.* **553**, 47 (2001).
- [38] G. Aldering, A. G. Kim, M. Kowalski, E. V. Linder, and S. Perlmutter, *ArXiv Astrophysics e-prints* (2006), astro-ph/0607030.
- [39] D. Huterer and M. S. Turner, *Phys. Rev. D* **64**, 123527 (2001), astro-ph/0012510.
- [40] W. Hu and B. Jain, *Phys. Rev. D* **70**, 043009 (2004).
- [41] A. Albrecht and G. Bernstein, *ArXiv Astrophysics e-prints* (2006), astro-ph/0608269.
- [42] H. Zhan and L. Knox, *Astrophys. J.* **644**, 663 (2006), astro-ph/0509260.
- [43] E. V. Linder, *Astroparticle Physics* **24**, 391 (2005).
- [44] D. N. Limber, *Astrophys. J.* **119**, 655 (1954).
- [45] N. Kaiser, *Astrophys. J.* **388**, 272 (1992).
- [46] W. Hu, *Astrophys. J. Lett.* **522**, L21 (1999).
- [47] M. Zaldarriaga and U. Seljak, *Astrophys. J. Suppl. Ser.* **129**, 431 (2000), astro-ph/9911219.